

# 40-GHz/150-ns Versatile Pulsed Measurement System for Microwave Transistor Isothermal Characterization

Jean-Pierre Teyssier, Philippe Bouysse, Zineb Ouarch, Denis Barataud, Thierry Peyretaillade, and Raymond Quéré, *Member, IEEE*

**Abstract**—A versatile pulsed  $I(V)$  and 40-GHz RF measurement system is described with all the know-how and methods to perform efficient, safe, and reliable nonlinear transistor measurements. Capability of discrimination between thermal and trapping effects with a pulse setup is demonstrated. Capture and emission constant times of trapping effects are measured. A method to electrically measure the thermal resistance and capacitance of transistors with a pulse setup is proposed.

**Index Terms**—Nonlinear RF characterization, pulsed measurements, thermal characterization, transistor.

## I. INTRODUCTION

SINCE the rising of efficient computer-aided design (CAD) tools for microwave circuits, the modeling activity has received a considerable interest in order to provide more reliable nonlinear models of microwave transistors to the active circuit designers. Especially in the case of up-to-date nonlinear high-performance amplifiers, mixers, multipliers, and dividers, the transistor model accuracy in the whole domain of operation is an absolutely necessary key point in order to achieve designs with first-pass success.

The modeling activity relies either on the physics of devices or measurements. In order to optimize their processes, physical-based models are of interest to component manufacturers. However, fast and reliable models for RF design based on device layer structures are not available today. Moreover, parasitics are difficult to describe as physical equations. At last, a physical-based model requires the knowledge of the device structure, not usually available for obvious reasons. On the other hand, measurement-based models take into account real-world devices including all the parasitics. Database optimizations and statistical approaches are used to ensure successful designs of monolithic microwave integrated circuits (MMIC's) [1]–[5].

The measurement approach requires to perform accurate, repeatable, and safe measurements of the devices. The fol-

Manuscript received November 20, 1997; revised July 24, 1998. This work was supported in part by the European Community under the ESPRIT 6016 “CLASSIC” program and by the Onera Cert Laboratory.

J.-P. Teyssier was with IRCOM, CNRS UMR 6615, University of Limoges, 19100 Brive, France. He is now with the University Institute of Technology (IUT), 19100 Brive, France.

P. Bouysse, Z. Ouarch, D. Barataud, and R. Quéré are with IRCOM, CNRS UMR 6615, University of Limoges, 19100 Brive, France.

T. Peyretaillade was with IRCOM, CNRS UMR 6615, University of Limoges, 19100 Brive, France. He is now with Alcatel Space, 31037 Toulouse, France.

Publisher Item Identifier S 0018-9480(98)09048-6.

lowing four main families of electrical measurements can be mentioned:

- 1)  $I(V)$ ;
- 2)  $S$ -parameters;
- 3) load-pull;
- 4) time domain.

The extensive knowledge of a device requires the use of each of these methods in order to extract the parameters of the model ( $I(V)$  and  $S$ -parameters) and to check its behavior in real operation (load-pull, time domain).  $I(V)$  and  $S$ -parameter measurements are usually performed under dc bias; in this case, the characterization procedure suffers from severe drawbacks, resulting in inaccuracies of the model. First, the dc power dissipated in the device causes self-heating effects, thus the temperature of characterization is not constant. Secondly, microwave FET's exhibit trapping effects that modify dc characteristics, inducing large errors in the determination of RF output conductance and transconductance [6]–[8]. Finally, dc nonsafe operation areas (such as breakdown) have to be investigated in order to provide a nonlinear model with all the boundaries that can be reached by large-signal RF.

All these drawbacks have motivated the development of measurement techniques based on pulses. They have received a considerable interest in the last few years; a number of pulsed  $I(V)$  or pulsed  $S$ -parameter systems have been proposed [9]–[15]. They rely on the measurement of  $I(V)$  and RF data during short rectangular pulses describing the characteristics around the dc bias point.

The goal of this paper is to describe an automatic measurement system performing simultaneously pulsed  $I(V)$  (two voltages and two currents) and pulsed  $S$ -parameters characterization for field effect and bipolar devices, with short pulse durations (width  $\geq 150$  ns) in a broad frequency range (500 MHz–40 GHz). In Section II, the pulsed  $I(V)$  measurement system is described. Section III is devoted to the pulsed  $S$ -parameter measurements. Finally, Section IV shows significant results of device investigation in terms of nonlinear behavior of transistors and discrimination of trapping and thermal effects of FET's. Measurement and extraction of thermal parameters are explained.

## II. PULSED $I(V)$ MEASUREMENTS

In order to provide suitable models for microwave CAD, the characterization of microwave devices should be realized with measurement conditions as close as possible to real-

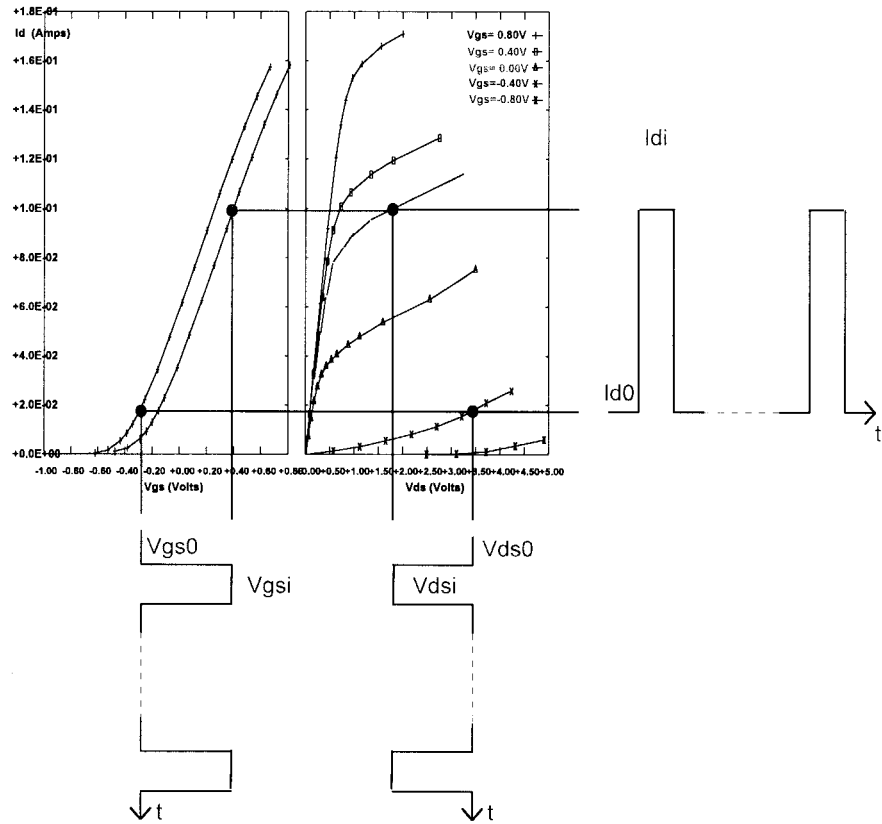


Fig. 1.  $I(V)$  pulse principle for an FET.

world operating conditions. Temperature time constants of microwave transistors are very large compared with the RF cycle. Thus, the device temperature does not change during a RF cycle; its drift depends on the average power dissipated inside the device. Since transistor characteristics strongly depend on device temperature, a realistic device characterization must be performed isothermally at a device temperature as close as possible to its real-world temperature.

#### A. Principle

Starting from the dc quiescent point, short pulses are used to describe the device behavior isothermally. Pulses from 150 ns to a few micrometers can be used, depending on the device. The measurement principle is shown in Fig. 1 for an FET.  $V_{gs0}$ ,  $V_{ds0}$ , and  $I_{d0}$  correspond to the quiescent point, and  $V_{gsi}$ ,  $V_{dsi}$ , and  $I_{di}$  are the pulsed-point values. Approximately 200 pulsed points are required around a dc bias point in order to plot the complete nonlinear input and output device characteristics.

#### B. Pulse Generators

Several pulse-generator technologies can be used for transistor characterization. We can mention classical 50- $\Omega$  pulse generators, 50- $\Omega$  arbitrary function generators, and high-power low-impedance pulsers. In all cases, a dc level not equal to zero capability is required for dc bias purpose. The generators are characterized by their internal resistance and their limitations in terms of voltage and/or current.

Pulse generators are driven by digital interfaces. Level steps of outputs are a drawback for achieving an accurate value of a current or voltage. The effect of quantization can be minimized by an external resistor divider if the output amplitude of the generator is much larger than required for the device-under-test (DUT).

Microwave transistors can exhibit output currents from a few milliamperes to several amperes under maximum voltages from a few volts up to more than 100 V. For that reason, changing a pulse generator must be easy in terms of software and hardware. At this time, we have: 1) two  $\pm 20$ -V 50- $\Omega$  pulse generators; 2) a  $-10$  to  $+40$ -V 7-A pulser; 3) a  $\pm 75$ -V 4-A pulse amplifier; and 4) a  $\pm 100$ -V 50- $\Omega$  pulser. Depending on the pulse-generator technology, transitions can be fixed, linear, Gaussian, or arbitrary. Fixed transitions frequently result in overshoots of  $I(V)$  slopes on the scope and can damage the device. When possible, Gaussian or linear transitions are preferable. Another way to limit overshoots consists in adding a small delay to the output port of device pulse and to reduce its width.

All combinations of these generators are possible; e.g., a pulser and an amplifier are used for high-power RF bipolar silicon transistor in a common base configuration. The software takes into account the generator various specifications with drivers providing a standardized library of commands.

#### C. Device Safety, Oscillation, and Biasing Network

A given transistor has absolute ratings provided by its manufacturer, and the pulse measurements can overrun these

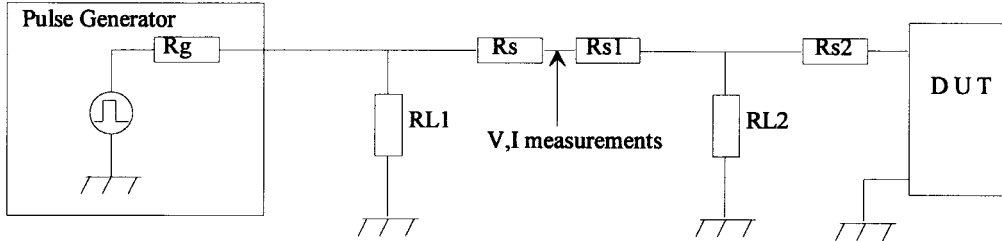


Fig. 2. Pulse generator and resistors for one port of the DUT.

ratings up to breakdown. Nevertheless, some limit values for voltages and/or current must be considered in order to ensure device safety. For that reason, virtual pulse generators with maximum-rating load lines adapted to the DUT limitations are required. They are realized with external resistors and values are limited by software for the generators.

Device oscillation may appear for some components, depending on the bias and pulsed point, impedances, gain, and test fixture. In the case of low-frequency oscillations, a change of external bias resistors or cable lengths can usually solve the problem. For high-frequency oscillations, a bias tee with a  $50\text{-}\Omega$  RF load or a tuner on its RF port can be used to provide an RF load to the device, but the  $I(V)$  pulses must pass through the bias tee; at least a 50-MHz cutoff frequency is required for the bias-tee dc path. If the bias tee has no sense port, the extra resistance of its inductance (from 0.1 to 0.75  $\Omega$ , depending on bias tees) is to be taken into account for  $I(V)$  measurements. Another method to stabilize a device consists of RF attenuators connected as close as possible to it. From the  $I(V)$  point-of-view, an RF attenuator is a set of three resistors in  $Y$  or  $\Pi$  configuration which have to be taken into account.

Thus, the matching resistor networks are optimized for each measurement configuration on each device port; this is a key-point task. It provides Thevenin or Norton impedance and steps of the virtual pulse generator adjusted to fit in the device capabilities and to ensure safety and oscillation avoidance.

A general network is proposed in Fig. 2 for one port of the device, defining a virtual pulse generator in the DUT planes.  $RL_1$  modifies the step and amplitude levels of the generator,  $R_s$  can be used for current limitation and measurement. The set of resistors  $R_{s1}$ ,  $R_{L2}$ , and  $R_{s2}$  is designed to take into account additional bias tees or attenuators. All the applied and measured levels are expressed as values in the DUT plane with a simple computation.

#### D. Pulse Timings

The shorter the pulses, the closer the device is to its RF behavior. The pulse duration and duty cycle must be adapted to the DUT as a compromise between the following points:

- 1) pulsedwidth must be large enough for quality of measurement acquisition;
- 2) pulsedwidth must be much smaller than the thermal time constant for isothermal characterization;
- 3) pulsedwidth must be smaller than the trapping time constant if traps exist;
- 4) pulse duty cycle must be large enough to ensure the thermal state is driven by the dc quiescent point;

- 5) pulse duty cycle must not be too large in order to ensure fast and reliable data acquisition with averaging.

A duty cycle of 0.1%–5% is usually acceptable, but it must be checked for each transistor. This can be done easily with a few measurement points [16], and the pulse durations have to be tested in the same manner. Pulsedwidth from 300 to 600 ns are usually suitable, but, from our experience, pulses as short as 150 ns are required for some millimetric high electron-mobility transistors (HEMT's) due to fast trapping effects (see results in Section IV).

#### E. $I(V)$ Measurements

The four electrical values are measured simultaneously during the pulse, with high accuracy for modeling purposes. This can be done either with a four-channel GPIB oscilloscope, or with VXI digitizers. From our experience, a screen display with the four pulse waveforms is very useful to check the measurements; overshoots, oscillations, heating, and other problems can be easily seen.

The measurement range is extremely large; for some devices, a base current of 1  $\mu\text{A}$  during pulses is under control, and we have measured collector or drain currents up to 7 A. Gate voltages are measured during pulses with an error smaller than 10 mV, drain voltages can reach 100 V for MOSFET's (this is not enough for SiC devices, etc.). Thus, probe technology and versatility of each manufacturer must be carefully considered when choosing a digitizer.

The voltage probes are classical high-impedance low-capacitance active or passive probes. For the currents, we have two configurations: differential probes associated with accurate external resistors ( $R_s$  in Fig. 2), and Hall probes. All combinations are available for the input and the output of transistors, depending on the current ranges.

#### F. $I(V)$ Accuracy and Calibration

Accurate  $I(V)$  characterization depends mainly on the offset accuracy of each input scaling factor given in the manufacturer specifications. The number of bits of the analog-to-digital converters is not so crucial if the scale is always set to its minimal value. Our system with its probes provides a specified dc voltage offset accuracy better than  $0.25\% \pm 5$  mV up to  $\pm 10$  V after warm-up and without averaging.

In order to optimize  $I(V)$  measurement accuracy of the device, external calibration of the setup is realized in conjunction with the scope or digitizer internal self-calibration. It consists of two one-path calibrations performed under pulsed

conditions with three high-quality broad-band standards (open, short,  $50 \Omega$ ) connected to the DUT ports. This calibration provides accurate values for  $R_{s1}$ ,  $R_{L2}$ ,  $R_{s2}$  on each port. If a RF attenuator is required for stability purposes, a large value of  $R_{s1} + R_{s2}$  or a small value of  $R_{L2}$  diminishes the  $I(V)$  measurement accuracy. Nevertheless, this technique is successfully used to take into account RF attenuators connected close to unstable devices in order to characterize them without oscillation.

The averaging technique can be used to improve the  $I(V)$  measurement accuracy, but it reduces the speed of the setup.

### G. Thermal Measurements

The temperature is a command of active devices. If the thermal resistance and thermal time constant of a device are known, harmonic-balance simulators can compute the device temperature and feed it back to the model [17]. Temperature measurements are made with the device put in a thermal enclosure, and its temperature should be controlled by software for extensive characterization.

### H. Measurement Algorithms

The overall software is a key point for fast and reliable device characterization under pulsed conditions. Due to the nonlinear nature of transistors, their current responses to the applied voltage levels are not easy to estimate in a general manner. Moreover, virtual pulse generators with resistances do not behave like pure voltage generators. Thus, when an electrical value must be reached, a careful predictive/corrective algorithm is required, e.g., to reach a  $V_{gs}$  value in conductive or breakdown region.

We have developed a set of algorithms based on electronic common sense with no *a priori* on a particular device behavior. This means that the code is written without any numerical constant depending on transistors because such a value always becomes a problem when a new family of transistor is tested. Thus, the same curve procedure is used for FET's  $V_{gs}$  or  $V_{ds}$  constant curves in hot or cold FET configuration and for bipolar  $I_b$  or  $I_e$  constant curves. This generalization is essential to the software reliability and flexibility.

The density of measured points is automatically adapted to the second-order derivative of characteristics, with a dichotomous recursive algorithm [18]. This method provides an optimization of the number of data points, each point is significant to the modeling activity. Moreover, it ensures a fast device characterization with a critical test of measurement accuracy.

An open database structure handles the measurements, and keeps the setup parameters embedded with them. This database provides a fast and efficient link with all modeling tools; this is a key point for fast and reliable design of models [3].

The conjunction of virtual generator boundaries and sophisticated measurement software (about 500 000 chars of C++) allows easy and very safe isothermal pulsed  $I(V)$  characterization of most RF transistors up to breakdown, conduction, or high-power regions. A batch mode is used for

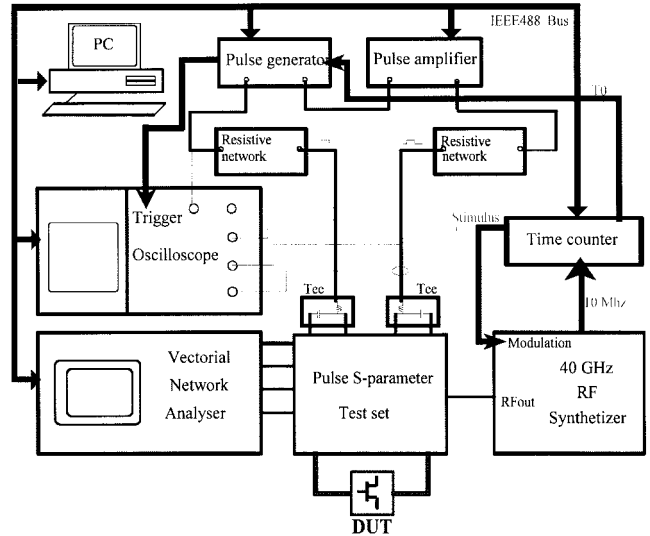


Fig. 3.  $I(V)$  and RF pulse setup.

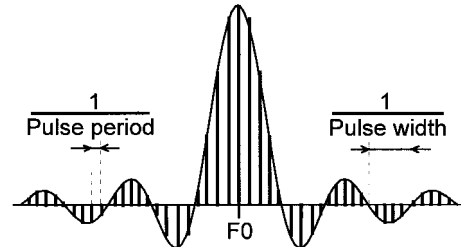


Fig. 4. Detected RF spectrum.

extensive characterization of devices (e.g., several dc points and/or several temperatures).

## III. PULSED S-PARAMETER MEASUREMENTS

Pulsed  $S$ -parameters are performed by superposition of RF stimulus and measurement during the  $I(V)$  pulses. A vectorial network analyzer (VNA) with short pulse ( $\leq 150$  ns) capabilities is required for isothermal measurement of transistors. With these pulse durations compared with RF frequencies, and with four identical measurement paths for the transmitted and reflected signals from the DUT to the samplers, the VNA quickly reaches a continuous wave (CW) mode during the pulses.

Bias tees with a dc bandpass allowing  $I(V)$  pulses connect the VNA to the  $I(V)$  setup, as shown in Fig. 3. A time synchronization between equipments places the RF measurements precisely during the  $I(V)$  pulses and avoids phase jitter.

### A. RF Pulsed Measurements

The RF source is modulated with an on/off rectangular stimulus signal provided by the time counter. The  $S$ -parameter measurements are acquired continuously, but the RF transmission and reflection signals are convoluted by this stimulus signal. Thus, the detected signals exhibit an infinite number of spectrum lines, as is shown in Fig. 4.

Two treatment methods of the RF signals can be used. Either the energy in the central frequency point of measure  $F_0$  is only taken into account with a narrow bandpass filter or a remix of

the lateral spectrum lines is performed in order to detect more energy. For practical reasons, these treatments are applied in test sets at an intermediate frequency. The second method is more difficult to implement because it needs two synchronized synthesizers, but it presents the advantage to provide twice more energy to the VNA detectors. In any case, the accuracy of a VNA in a CW mode is unreachable because in the pulse mode, the average RF energy injected in the DUT is divided by the duty cycle.

### B. RF Power Level

On the one hand, in order to perform small-signal (i.e., linear)  $S$ -parameters measurements of active components, the RF level at the DUT planes has to be small. On the other hand, an insufficient RF level brings measurements near to the VNA noise level. This is a critical point for RF pulsed measurement at high frequencies, due to the overall system losses and the decrease of energy caused by the pulses. A careful control of the RF level of the synthesizer, usually not performed for CW measurements, ensures the linear condition and minimizes the problem of the measurement level.

A power meter connected to DUT planes before calibration allows us to drive the source level for each frequency to achieve an RF flat-power level versus frequencies. Moreover, we insert an attenuator in the VNA port-1 path before calibration; thus, port 2 (drain or collector) incident levels are higher than port 1 (gate or base), inducing a better accuracy for the very small scattering parameter  $S_{12}$ .

Depending on device technology and size, RF power levels in the DUT planes from  $-12$  to  $-21$  dBm are suitable for small-signal  $S$ -parameter measurements. This level is checked by biasing the device in a nonlinear region (usually at pinchoff for FET's) and by monitoring the trace on the oscilloscope: if the RF level is set too high, the drain current increases by self-biasing during the RF pulse. Moreover, this test is a good way to check the RF pulse position versus the  $I(V)$  pulses.

### C. RF Calibration

All classical calibration methods are available for our pulse measurements, with their respective advantages and drawbacks (Standard, LRL, LRM, LRRL with SMA, K, alumina or on-wafer connections).<sup>1</sup> [19], [20] Thus, trackability of RF pulsed measurements versus referenced standards is available.

We can calibrate either in CW or in pulse mode. Our best results in terms of pulsed device measurement accuracy are obtained with calibrations performed in pulse mode at  $-10$ -dBm flat-power level. This is due to the VNA detected levels during the calibration that are close to the detected levels when the DUT is connected, reducing the VNA linearity error effects on measurements.

In spite of the smaller energy available at the VNA detectors due to pulses, good measurement results up to 40 GHz at an RF measurement flat level of  $-15$  dBm and a 2.5% duty cycle with 150-ns measurements width allow direct extraction of a device equivalent scheme (see Section IV).

<sup>1</sup>“Measurement calibration,” Model 360B vector network analyzer system, Wiltron manual, release 4.01, Morgan Hill, CA, 1991.

This performance is achieved with our VNA test set modified in order to dispose of reference signals with enough level to phase-lock local intermediate frequency (IF) oscillators. This enhancement avoids the use of a phase-lock mode based on a 10-MHz reference signal.

## IV. MEASUREMENT RESULTS

### A. FET Results

First, we will propose results to show 40-GHz measurement accuracy. Then, trapping effects will be exhibited, separated from thermal effects. Finally, measurement of thermal resistance and thermal time constant will be demonstrated.

In order to demonstrate pulsed RF measurement accuracy, the measured and modeled real and imaginary  $S$  parameters of an on-wafer 0.20- $\mu\text{m}$  HEMT are proposed in Fig. 5. The calibration method is LRM with Cascade ISS kit. The modeled parameters are obtained instantaneously by direct extraction from the 40-GHz pulsed RF measurements, without optimization [21].

Trapping effects of FET's induce a dispersive behavior of the drain current. The captured charges in DX centers versus the bias are exhibited by three  $I(V)$  pulsed measurements starting from three different dc bias point, performed with the same dissipated dc power (on the 250-mW hyperbola), as shown in Fig. 6.

With a dc bias point and a pulsed point placed on the same output power hyperbola, i.e., at the same temperature, we observe the capture and emission times of traps on the oscilloscope. This is shown in Fig. 7 with a constant dissipated power of 37 mW and a large pulse on voltage divider switching (VDS) from 1 to 8.6 V. We can mention in this measurement example that trap capture is very fast compared with traps emission. We can notice that the gain is much larger at low frequencies than at RF frequencies. Pulsed  $I(V)$  measurements performed with very short pulses are consistent with the RF behavior of devices from the trapping effect point-of-view.

Thermal resistance of FET's can be measured electrically with a pulse setup by a method based on Fukui [9]. The Schottky gate-to-source diode is used as an embedded thermometer. The key point consists in assuming that trapping effects are essentially due to  $V_{ds}$  voltage. Thus, we choose and hold a  $V_{ds0}$  value for the complete process. The first step calibrates the gate diode embedded thermometer for a given  $I_{gm}$  pulsed gate current with a thermal enclosure without any dc power dissipated in the transistor. Slopes from  $-1$  to  $-1.4$  mV/K are obtained for AsGa [see Fig. 8(a)]. Then, power is dissipated in the device, and the short pulses are used to acquire isothermally the value of  $V_{gs}$  for the given gate current  $I_{gm}$ . The temperature versus the dissipated power is plotted [see Fig. 8(b)], its slope is the thermal resistance. This value has been successfully checked with other sets of ( $V_{ds0}$ ,  $I_{gm}$ ).

Thermal simulations of nonlinear devices need to integrate the dissipated power versus time in order to compute the device temperature. Thus, a thermal time constant must be considered: the so-called transistor thermal capacitance. The

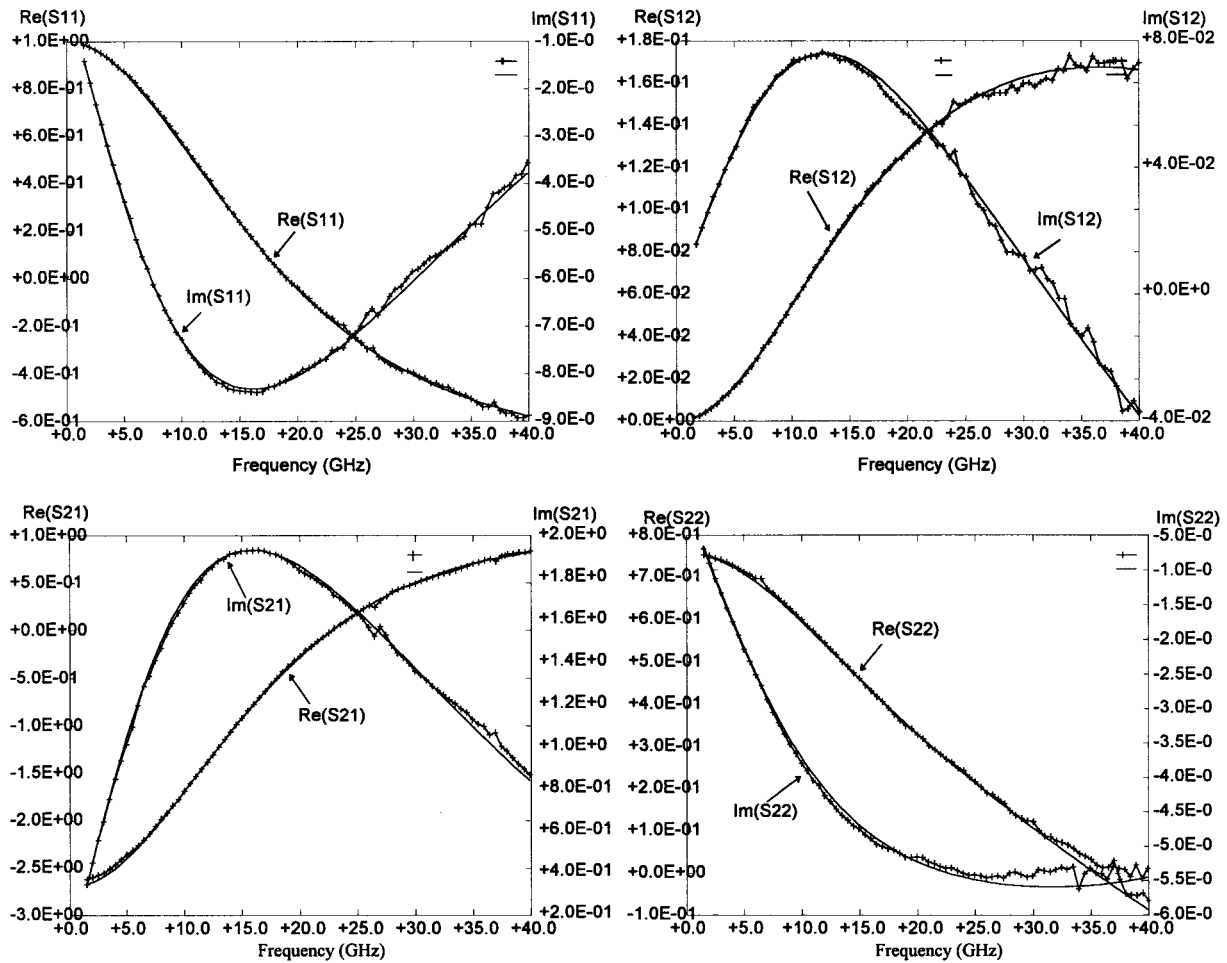


Fig. 5. Pulsed RF measurement and model, HEMT VLN02  $\times 4 \times 50 \mu\text{m}$ , pulselength: 150 ns, pulse period: 6  $\mu\text{s}$ .

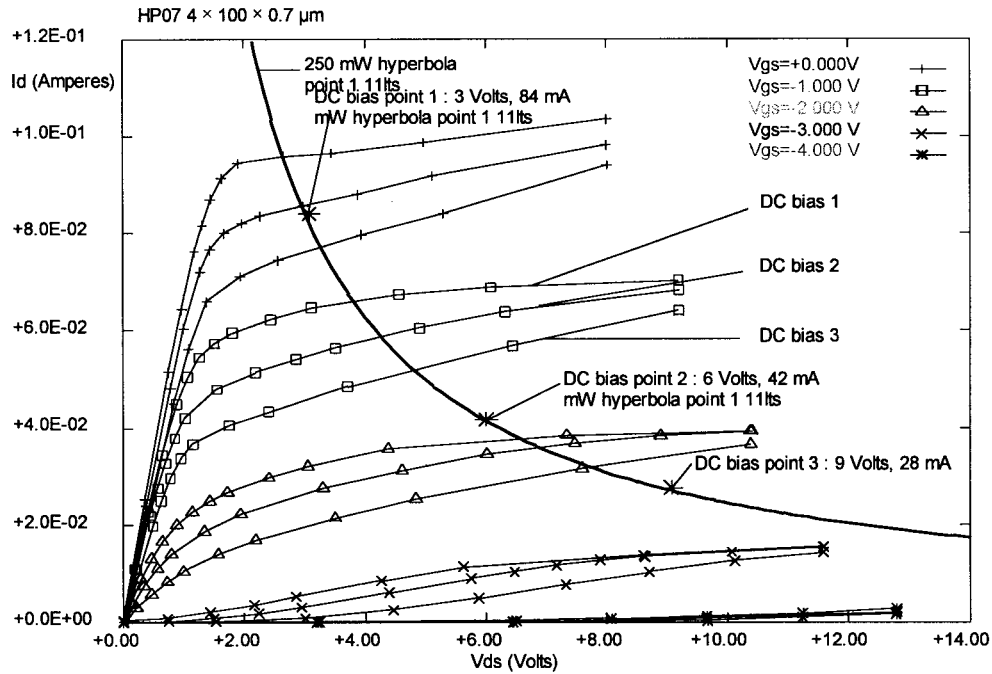


Fig. 6. Three isothermal output characteristics of an HP07  $4 \times 100 \times 0.7 \mu\text{m}$  FET.

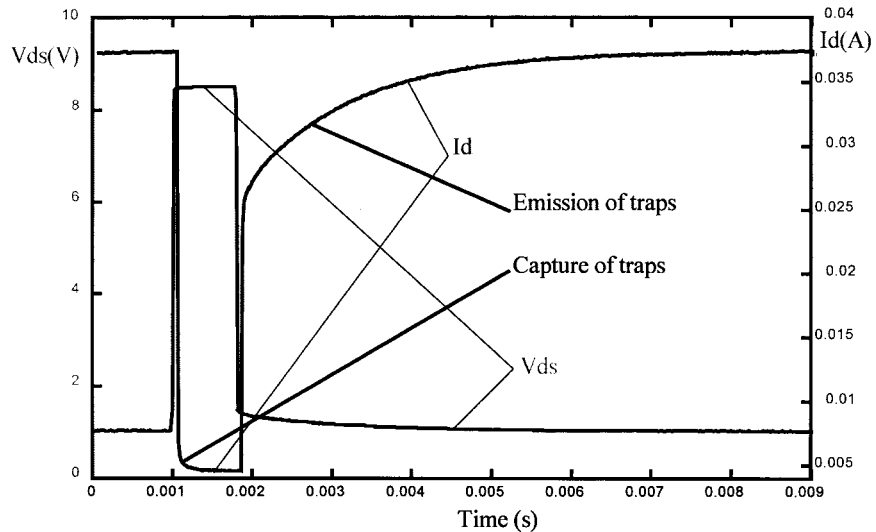


Fig. 7. Capture and emission of traps, MESFET  $0.7 \mu\text{m} \times 4 \times 100 \mu\text{m}$ , at a constant dissipated power of 37 mW.

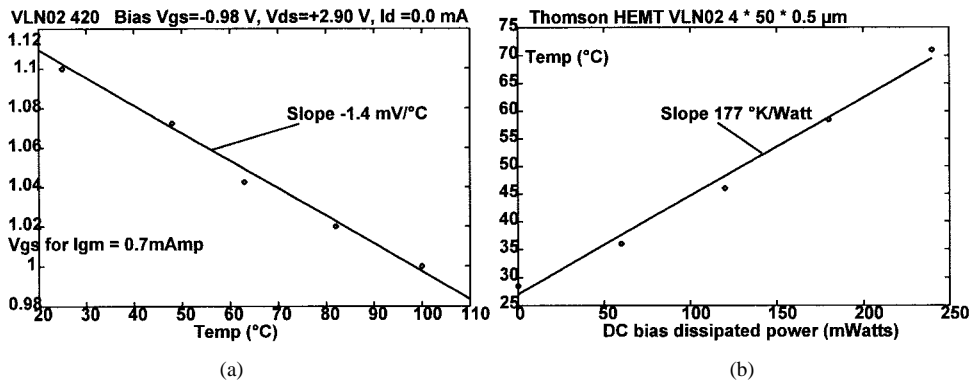


Fig. 8. (a) Gate diode threshold voltage versus temperature:  $-1.4 \text{ mV/K}$ . (b) Temperature versus dc dissipated power:  $R_{\text{th}} = 177 \text{ K/W}$ .

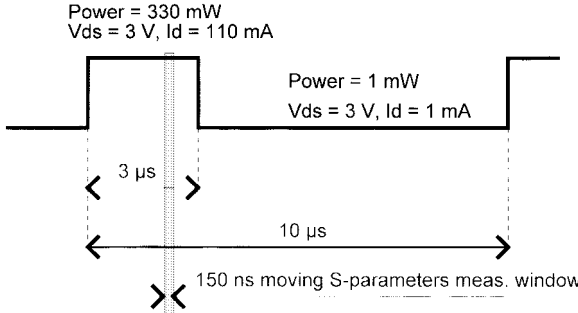


Fig. 9. Heating/cooling cycle of  $\text{VLN02 } 4 \times 50 \mu\text{m}$  transistor, 150-ns measurement shifting window.

pulse  $I(V)$  and pulse RF setup offers a way to achieve the determination of this element. The gain of FET devices depends on the temperature, and this dependence is considered linear for limited heatings. The gain is measured with the pulsed VNA during a 150-ns window of time that we move along a cycle of heating/cooling applied with  $I(V)$ , as shown in Fig. 9.

$S_{21}$  magnitude versus time during the cycle is plotted and fitted with an exponential equation. This leads to a 650-ns time constant (see Fig. 10).

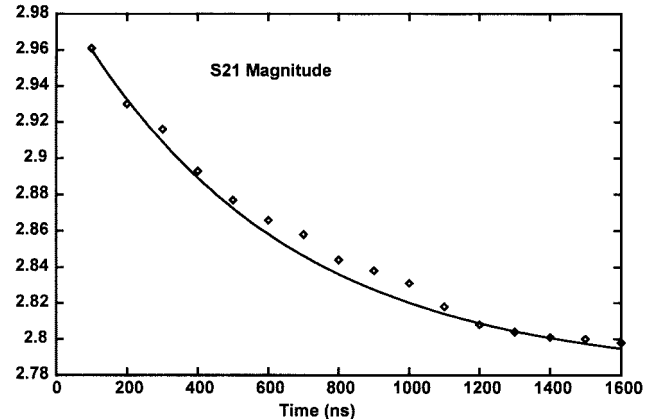


Fig. 10. Decrease of the gain versus temperature during the device heating.

The same study is performed with the cooling of the device where slightly longer time constants are obtained. This is due to the fact that a thermal model with only one thermal resistance and one capacitance is very simple; more thermal cells should be considered to take into account the vicinity of the channel. Nevertheless, this measurement technique is very realistic for thermal modeling of devices used in non-

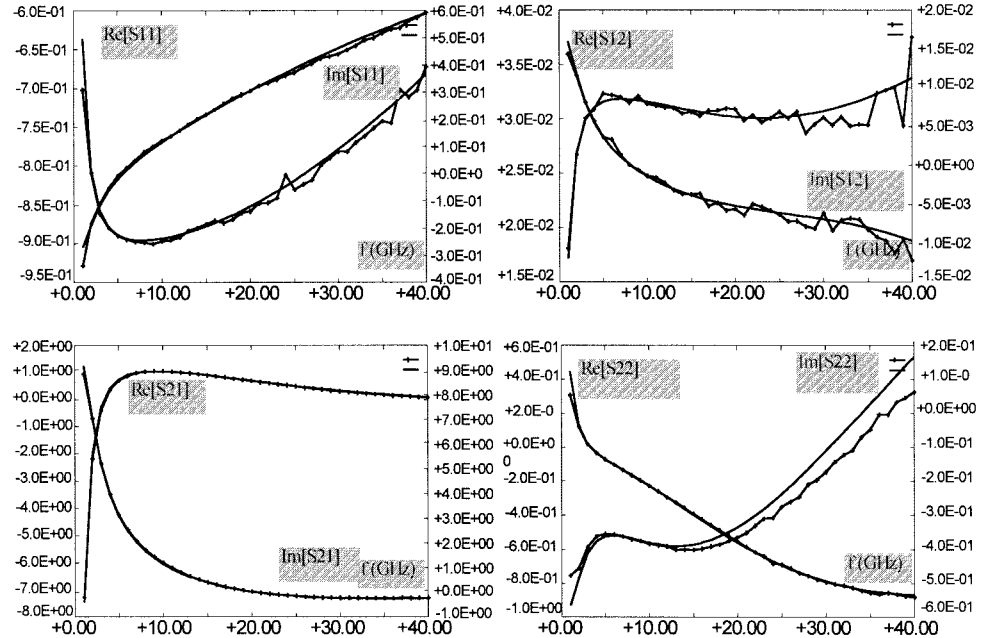


Fig. 11. HBT pulsed  $S$ -parameters measurements and model  $6 \times (2 \times 30) \mu\text{m}^2$  GaInP/GaAs  $V_{\text{ceo}} = 8.5$  V;  $I_{\text{co}} = 75$  mA; pulselength: 150 ns, pulse period: 6  $\mu\text{s}$ .

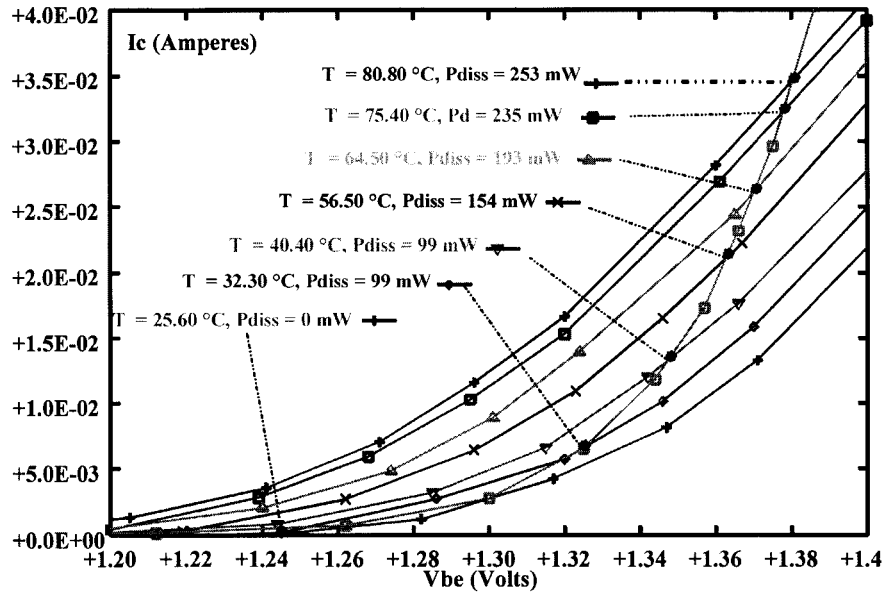


Fig. 12. Measured and modeled HBT drain current for  $V_{\text{ce}} = 7$  V.

CW applications because we use a measure of the channel characteristics versus the power dissipated in the channel.

#### B. Bipolar Transistor Results

Bipolar transistors are affected by strong temperature effects: HBT's collector current decrease with temperature, and silicon devices current increase dangerously with temperature. Multifinger HBT's exhibit collapses of current due to the differences of temperature between fingers, inducing conditional thermal instabilities of devices [22], [23]. Thus, isothermal characterizations are indispensable; moreover, the short  $I(V)$  pulses can investigate the current collapse area.

In order to show pulsed on-wafer RF measurement accuracy of bipolar transistors, pulsed  $S$ -parameters and modeled parameters up to 40 GHz of a  $6 \times (2 \times 30) \mu\text{m}^2$  GaInP/GaAs heterostructure bipolar transistor (HBT) device are proposed in Fig. 11.

Fig. 12 shows the collector current at fixed  $V_{\text{ce}}$  versus  $V_{\text{be}}$  for different bias points. A thermal model of the collector current has been developed and is plotted in the same figure, and the device temperature is calculated with its thermal resistance. The thermal resistance has been obtained with the pulse setup in the same manner as FET's (base-emitter diode thermometer) [24].

The accuracy of HBT pulsed  $S$ -parameters allows direct extraction of the equivalent circuit of the device and integration of this circuit versus device commands in order to achieve a nonlinear and thermal model of the overall transistor, with thermal instabilities taken into account.

### C. Measurement Consistency and Other Results

The measurement consistency check of pulsed  $I(V)$  derivatives versus pulsed  $S$ -parameters is systematically performed in the whole working domain of transistors. For FET's, we compare  $g_m$  and  $g_d$  with  $I(V)$  drain current derivatives and, for bipolar devices, we compare

$$gm_0R_{be} = \beta$$

with

$$R_{be} = \left( \frac{\partial I_b}{\partial V_{be}} \right)^{-1}$$

A large number of other significative results in terms of various device characterization (MOSFET, SiC, pMHFET) and device modeling (breakdown, distributed models, etc.) have been obtained with the versatile pulsed  $S$ -parameters measurement setup and have been published in [25]–[27].

## V. CONCLUSION

The new transistor pulsed measurement features proposed in this paper (higher frequencies with very short pulses) open new perspectives for the electrical and thermal characterization of high-frequency nonlinear devices. We demonstrate the capability to separate thermal and trapping effect characterization with a pulsed setup; this feature is essential in order to achieve reliable thermal models and to improve our knowledge of nonlinear devices.

The  $I(V)$  and RF pulsed equipments have proven that they are essential tools to perform accurate nonlinear and isothermal measurements of microwave transistors, allowing accurate and efficient model extraction. It is now obvious that pulsed measurements of active devices are absolutely necessary for designers to achieve first-pass design success of high-performance nonlinear MMIC's.

The know-how and software associated with this equipment have been sold, and has been updated since 1993. It is currently used daily in five industrial or research companies. More than 1000 different microwave transistors (MESFET's, HEMT's, pMHFETs, MOSFET's, Bip Si, HBT's, SiC, etc.) have been successfully measured. A large number of RF circuit designs based on our pulsed measurements of transistors have been realized, reflecting very good confidence in results.

### ACKNOWLEDGMENT

The authors want to thank J. Favre, S. L. Delage, and P. Auxemery, Thomson, Orsay, France, for providing the tested devices, and Prof. J. Obregon for helpful discussions.

## REFERENCES

- [1] D. E. Root, "Measurement-based active device modeling for circuit simulation," presented at the EuMC Workshop, Madrid, Spain, 1993.
- [2] J. W. Bandler, S. H. Chen, S. Daijivad, "Microwave device modeling using efficient  $l_1$  optimization: A novel approach," *IEEE Trans. Microwave Theory Tech.*, vol. MTT-34, pp. 1282–1293, Dec. 1986.
- [3] R. Quéré, J. Obregon, and J. P. Teyssier, "Non linear characterization and modeling of semi-conductor devices: An integrated approach," in *23th European Microwave Conf. Workshop*, Madrid, Spain, 1993, pp. 18–21.
- [4] R. Quéré, J. M. Nébus, J. P. Villette, and J. Obregon, "A complete, measurement based, methodology for the extraction and verification of nonlinear models of active devices," presented at the IEEE Workshop Experimentally-Based FET Device Modeling & Related Nonlinear Circuit Design, Kassel, Germany, 1997.
- [5] A. Werthof, F. van Raay, and G. Kompa, "Direct nonlinear power MESFET parameter extraction and consistent modeling," in *IEEE Microwave Theory Tech. Symp. Dig.*, Atlanta, GA, 1993, pp. 645–648.
- [6] J. M. Golio, M. G. Miller, G. N. Maracas, and D. A. Johnson, "Frequency-dependant electrical characteristics of GaAs MESFET's," *IEEE Trans. Electron Devices*, vol. 37, pp. 1217–1227, May 1990.
- [7] G. I. Ng and D. Pavlidis, "Frequency-dependant characteristics and trap studies of lattice-matched ( $x = 0.53$ ) and strained ( $x > 0.53$ )  $In_{0.52}Al_{0.48}As/In_xGa_{1-x}As$  HEMT's," *IEEE Trans. Electron Devices*, vol. 38, pp. 862–870, Apr. 1991.
- [8] F. Filicori, G. Vannini, A. Mediavilla, and A. Tazon, "Modeling of deviations between static and dynamic drain characteristics in GaAs FET's," in *EMC Conf.*, Madrid, Spain, 1993, pp. 454–457.
- [9] H. Fukui, "Thermal resistance of GaAs field-effect transistors," *IEEE Trans. Electron Devices*, vol. ED-5, pp. 118–121, 1980.
- [10] T. M. Barton, C. M. Snowden, J. R. Richardson, and P. H. Ladbrooke, "Narrow pulse measurement of drain characteristics of GaAs MESFET's," *Electron Lett.*, vol. 23, pp. 686–687, 1987.
- [11] M. Paggi, P. H. Williams, and J. M. Borrego, "Nonlinear GaAs MESFET modeling using pulsed gate measurements," *IEEE Trans. Microwave Theory Tech.*, vol. 36, pp. 1593–1597, June 1988.
- [12] A. Platzker, A. Palevski, S. Nash, W. Strubble, and Y. Tajima, "Characterization of GaAs devices by a versatile pulsed  $I-V$  measurement system," in *IEEE MTT-S Symp. Dig.*, Dallas, TX, May 1990, pp. 1137–1140.
- [13] J. F. Vidalou, J. F. Grossier, M. Chaumas, M. Camiade, P. Roux, and J. Obregon, "Accurate nonlinear transistor modeling using pulsed parameters measurements under pulsed bias conditions," in *IEEE MTT-S Symp. Dig.*, Boston, MA, 1991, pp. 95–99.
- [14] J. P. Teyssier, M. Campoccchio, C. Sommet, J. Portilla, and R. Quéré, "A pulsed  $S$  parameter measurement set up for the nonlinear characterization of FET's and bipolar power transistors," in *EuMC Dig.*, Madrid, Spain, 1993, pp. 489–494.
- [15] J. Scott, M. Sayed, P. Schmitz, and A. Parker, "Pulsed-bias/pulsed RF device measurement system requirements," in *EMC Dig.*, Cannes, France, 1994, pp. 951–961.
- [16] A. Parker, J. Scott, J. Rathmell, and M. Sayed, "Determining timing for isothermal pulsed-bias  $S$ -parameters measurements," in *IEEE MTT-S Symp. Dig.*, Orlando, FL, May 1996, pp. 1707–1710.
- [17] R. Sommet, T. Peyretailade, A. Mallet, J. P. Teyssier, and R. Quéré, "A CAD electrothermal model for the nonlinear simulation of high power silicon bipolar transistors," in *INMMC 96*, Duisburg, Germany, 1996, pp. 102–107.
- [18] J. P. Teyssier, J. P. Viaud, J. J. Raoux, and R. Quéré, "Fully integrated nonlinear modeling and characterization system of microwave transistors with on-wafer pulsed measurements," in *IEEE MTT-S Symp. Dig.*, Orlando, FL, May 14–19, 1995.
- [19] D. Ryting, "An analysis of vector measurement accuracy, enhancement techniques," Tech. Note, Hewlett-Packard Company, Santa Rosa, CA.
- [20] H. J. Eul and B. Shiek, "A generalized theory and new calibration procedures for network analyzer self-calibration," *IEEE Trans. Microwave Theory Tech.*, vol. 39, pp. 724–731, Apr. 1991.
- [21] G. Dambrine, A. Cappy, F. Héliodore, and E. Playez, "A new method for the FET small-signal equivalent circuit," *IEEE Trans. Microwave Theory Tech.*, vol. 36, pp. 1151–1159, July 1988.
- [22] L. L. Liou, B. Bayraktaroglu, and C. I. Huang, "Thermal stability of multiple emitter finger microwave AlGaAs/GaAs heterojunction bipolar transistors," in *IEEE Microwave Theory Tech. Symp. Dig.*, Atlanta, GA, 1993, pp. 281–284.
- [23] W. Liu and A. Khatibzadeh, "The collapse of current gain in multifinger HBT's operated at very high power densities," *IEEE Trans. Electron Devices*, vol. 40, no. 11, pp. 1698–1707, Nov. 1993.

- [24] T. Peyretailade, M. Perez, S. Mons, R. Sommet, P. Auxemery, J. C. Lalaurie, and R. Quéré, "A pulsed-measurement based electrothermal model of HBT with thermal stability prediction capabilities," in *IEEE Microwave Theory Tech. Symp. Dig.*, Denver, CO, 1997.
- [25] J. P. Teyssier, J. P. Viaud, and R. Quéré, "A new nonlinear  $I(V)$  model for FET including breakdown effects," *IEEE Microwave Guided Wave Lett.*, vol. 4, pp. 104–106, Apr. 1994.
- [26] J. M. Colliantes, J. J. Raoux, J. P. Villette, R. Quéré, G. Montoriol, and F. Dupis, "A new large-signal model based on pulse measurement techniques for RF power MOSFET," in *IEEE Microwave Theory Tech. Symp. Dig.*, Orlando, FL, 1995.
- [27] B. Mallet-Guy, Z. Ouarch, M. Prigent, R. Quéré, and J. Obregon, "A distributed, measurement based, nonlinear model of FET's for high frequencies applications," in *IEEE Microwave Theory Tech. Symp. Dig.*, Denver, CO, 1997.

**Jean-Pierre Teyssier** received the Master degree in electronics and the Ph.D. degree from the University of Limoges, Limoges, France, in 1988 and 1994, respectively.

His developed a pulsed measurement setup devoted to the nonlinear characterization of microwave transistors at the Research Institute of Microwave and Optical Communications, IRCOM, Limoges, France. In 1995, he joined the University Institute of Technology (IUT), Brive, France, where he works on the characterization and modeling of nonlinear devices.

**Philippe Bouysse** was born in Aurillac, France, in September 1965. He received the Ph.D. degree in communication engineering from the University of Limoges, Limoges, France, in 1992.

Since 1992, he has been with the Microwave Laboratory, University of Limoges. His main interest is the characterization and nonlinear modeling of microwave transistors.

**Zineb Ouarch** received the Master's degree in electronics from Brest University, Brest, France, in 1995, and is currently working toward the Ph.D. degree in electronics.

In 1996, she joined the Research Institute of Microwave and Optical Communications of Limoges, IRCOM, Limoges, France, where she has worked on developing GaAs FET nonlinear models from pulsed measurements.

**Denis Barataud** was born in Saint-Junien, France, on October 5, 1970. He graduated from Ecole Nationale Supérieure de Télécommunications de Bretagne, Brest, France, in 1994, and is currently working toward the Ph.D. degree in electronic engineering at the University of Limoges, Limoges, France.

Since 1995, he has been with the Microwave Laboratory, University of Limoges. His main research interest is the time-domain characterization of nonlinear devices.

**Thierry Peyretailade** received the Master degree in electronics and the Ph.D. degree from the University of Limoges, Limoges, France, in 1994 and 1997, respectively.

From 1994 to 1997, he was with the Research Institute of Microwave and Optical Communications, IRCOM, Limoges, France, where he was involved with nonlinear electrothermal modeling of heterojunction bipolar transistors (HBT's) and high-efficiency power-amplifier design. In April 1998, he joined Alcatel Space, Toulouse, France, where he is an Equipment Design Engineer.

**Raymond Quéré** (M'88) received the engineer and French "agregation" degrees in applied physics from ENSEEIHT Toulouse, Toulouse, France, in 1976 and 1978, respectively, and the Ph.D. degree from the University of Limoges, Limoges, France, in 1989.

In 1989, he was appointed Professor at the Technology Institute of Electrical Engineering (IUT), Brive, France, where he is involved in research dealing with nonlinear design and modeling of microwave circuits, with a special emphasis on nonlinear stability analysis of potentially unstable circuits such as oscillators, frequency dividers, and power amplifiers. He is also strongly involved with nonlinear characterization and modeling of microwave active devices based on pulsed measurements techniques.

Dr. Quéré is a member of the Technical Committee of the EuMC. He has served as a reviewer for the IEEE TRANSACTIONS ON MICROWAVE THEORY AND TECHNIQUES.